Published in final edited form as:
Exp Neurol. 2012 January ; 233(1): 205–213. doi:10.1016/j.expneurol.2011.09.037.

Opiate agonist-induced re-distribution of Wntless, a mu-opioid receptor interacting protein, in rat striatal neurons

B. A. S. Reyes[1], **K. Vakharia**[1], **T. N. Ferraro**[3], **R. Levenson**[2], **W. H. Berrettini**[3], and **E. J. Van Bockstaele**[1]

[1]Department of Neuroscience, Farber Institute for Neurosciences, Thomas Jefferson University, Philadelphia, PA 19107

[2]Department of Pharmacology, Penn State College of Medicine, Hershey, PA 17033

[3]Department of Psychiatry, Center for Neurobiology and Behavior, University of Pennsylvania School of Medicine, Philadelphia, PA 19104

Abstract

Wntless (WLS), a mu-opioid receptor (MOR) interacting protein, mediates Wnt protein secretion that is critical for neuronal development. We investigated whether MOR agonists induce re-distribution of WLS within rat striatal neurons. Adult male rats received either saline, morphine or [D-Ala_2, N-Me-Phe_4, Gly-ol_5]-enkephalin (DAMGO) directly into the lateral ventricles. Following thirty minutes, brains were extracted and tissue sections were processed for immunogold silver detection of WLS. In saline-treated rats, WLS was distributed along the plasma membrane and within the cytoplasmic compartment of striatal dendrites as previously described. The ratio of cytoplasmic to total dendritic WLS labeling was 0.70±0.03 in saline-treated striatal tissue. Morphine treatment decreased this ratio to 0.48±0.03 indicating a shift of WLS from the intracellular compartment to the plasma membrane. However, following DAMGO treatment, the ratio was 0.85±0.05 indicating a greater distribution of WLS intracellularly. The difference in the re-distribution of the WLS following different agonist exposure may be related to DAMGO's well known ability to induce internalization of MOR in contrast to morphine, which is less effective in producing receptor internalization. Furthermore, these data are consistent with our hypothesis that MOR agonists promote dimerization of WLS and MOR, thereby preventing WLS from mediating Wnt secretion. In summary, our findings indicate differential agonist-induced trafficking of WLS in striatal neurons following distinct agonist exposure. Adaptations in WLS trafficking may represent a novel pharmacological target in the treatment of opiate addiction and/or pain.

Introduction

Wnts belong to a family of secreted glycoproteins essential for cell signaling, development and physiological processes (Jin et al., 2010; Logan and Nusse, 2004; Lie et al., 2005; Fu et al., 2009). As extracellular signaling molecules, Wnt proteins possess neurotrophic properties (Ciani and Salinas, 2005; Banziger et al., 2006). Specifically in neuronal

Corresponding Author: Beverly A. S. Reyes, D.V.M., Ph.D., Department of Neuroscience, Farber Institute for Neurosciences, Thomas Jefferson University, 900 Walnut Street, Suite 400, Philadelphia, PA 19107, Voice: (215) 503-5857, FAX: (215) 503-9238, bsr103@jefferson.edu.

development, Wnt proteins have been shown to stimulate synapse formation and dendritic morphogenesis, in addition to controlling axon pathfinding, remodeling and guidance (Ciani and Salinas, 2005), indicating that Wnt proteins regulate diverse neuronal functions. Biochemical and genetic analyses have shown that perturbations in Wnt signaling have been implicated in various diseases (Logan and Nusse, 2004; Grigoryan et al., 2008). For example, dysregulation of Wnt and its signal transduction cascade may contribute to the development of malignancies in various organs (Clevers, 2006).

A conserved gene that is essential for Wnt secretion was identified in *Drosophila* named Wntless or evenness interrupted or Sprinter (Banziger et al., 2006; Bartscherer et al., 2006; Goodman et al., 2006; Jin et al., 2010a, 2010b; Reyes et al., 2010). The Wntless/Evenness interrupted/Sprinter gene encodes a multi-pass transmembrane protein that is conserved from worms to human and is a vital component for Wnt secretion in *Drosophila* (Banziger et al., 2006; Bartscherer et al., 2006; Franch-Marro et al., 2008). WLS is the mammalian ortholog of *Drosophila* Wntless/Evenness interrupted/Sprinter. WLS protein is also known as GPR177 (Jin et al., 2010a, 2010b; Reyes et al., 2010). We have recently identified it as a mu-opioid receptor (MOR) interacting protein that may possibly serve as a substrate underlying the alterations in neuronal structure and synaptic organization characteristic of opioid dependence (Jin et al., 2010a).

Upon chronic exposure to a MOR agonist such as morphine or heroin, opiates exert inhibitory effects on axon outgrowth, dendritic arborization, and neurogenesis in brain regions known to be involved in reward processing, as well as learning and memory (Ciani and Salinas, 2005). Using immunoelectron microscopy, we have recently shown that WLS and MOR are co-localized in somata and in dendritic processes in the murine striatum (Jin et al., 2010a; Reyes et al., 2010), a brain region which is also involved in goal oriented behaviors and extrapyramidal motor control (Watson and Stanton, 2009; Kehagia et al., 2010). We demonstrated that 32% of WLS-labeled dendrites contained MOR immunoreactivity while 37% of MOR-labeled profiles contained WLS immunoreactivity (Reyes et al., 2010). It has recently been shown that proteins that interact directly with the MOR influence MOR biosynthesis, trafficking and signaling (Milligan, 2005), suggesting that MOR interacting proteins could regulate multiple mechanisms including signaling and trafficking. The mechanism underlying MOR desensitization or internalization may vary according to agonist exposure (Van Bockstaele and Commons, 2001; Bailey et al., 2003; Bailey et al., 2004; Bailey and Connor, 2005). Thus, in the present study, we examined whether the opiate agonists morphine or [D-Ala_2, N-Me-Phe_4, Gly-ol_5]-enkephalin (DAMGO) cause a redistribution of WLS in striatal neurons using high resolution immunoelectron microscopic analysis. Morphine and DAMGO were selected because morphine causes little MOR internalization (Van Bockstaele and Commons, 2001; Keith et al., 1996), while DAMGO causes significant receptor internalization (Johnson et al., 2006).

Experimental Procedures

Animals

Fifteen adult male Sprague-Dawley rats (Harlan Sprague Dawley Inc., Indianapolis, IN, USA; 250–270g) housed two to three to a cage (20°C, 12-h light, 12-h dark cycle lights on 0700) were used in this study. They were allowed ad libitum access to standard chow and water. All procedures were approved by The Institutional Animal Care and Use Committee at Thomas Jefferson University according to the revised *Guide for the Care and Use of Laboratory Animals* (1996), The Health Research Extension Act (1985) and the PHS Policy on Humane Care and Use of Laboratory Animals (1986). All efforts were made to utilize only the minimum number of animals necessary to produce reliable scientific data, and experiments were designed to minimize any animal distress.

Specificity of antisera

Anti-WLS antibody was generated in chickens against a peptide antigen corresponding to the C-terminal 18 amino acids (HVDGPTEIYKLTRKEAQE) of human WLS (Gene-Tel Laboratories, Madison, WI), which is identical to the rat and mouse peptide sequence. Antibodies of the IgY subtype were harvested from egg yolks and affinity purified prior to use. The characterization and specificity of the chicken antiserum against WLS has been previously described (Jin et al., 2010a). Western blot analysis using WLS antibody showed expression of the WLS in rat brain lysates indicating that WLS antibody recognized endogenous WLS in brain tissue. WLS recognized single band of proteins with approximate molecular weight of about 50kDa (Jin et al., 2010a). Omission of the primary antibody abolished any detectable immunoreactivity (Reyes et al., 2010).

Western Blot

To further characterize specificity of WLS antibody, brain tissue from frontal cortex was harvested isolated, frozen on dry ice and stored at −80C until analyzed. Tissue was weighed, homogenized in TRIzol® Reagent (Invitrogen, Carlsbad, CA) and combined with 5 volumes of chloroform. Centrifugation at 12,000 × g facilitated separation of aqueous (RNA) and organic phases (DNA/Protein). Protein was precipitated with ethanol, pellets were vacuum-dried and re-suspended in 1% SDS. Protein levels were quantified using Pierce BCA Protein Assay Kit (ThermoScientific g of protein were separated on a NuPage 4–12%μ Product No. 23225) and 50 gradient Bis-Tris gel. Separated proteins were transferred onto a nitrocellulose membrane with the use of an iBlot® Dry Blotting System (Invitrogen, Carlsbad, CA). The primary antibody solution contained chicken anti-WLS antibody at a 1:4500 dilution in 5% dry milk. The blocking peptide solution contained chicken anti-WLS antibody (1:4500 dilution) together with the WLS blocking peptide (1:1000 dilution) in 5% dry milk. Solutions were incubated overnight at 4°C with gentle agitation. Nitrocellulose membranes containing blotted proteins were blocked for 1 hour in 10% dry milk at room temperature and incubated with primary antibody solution or blocked (i.e. with peptide) primary antibody solution, also at room temperature for 1 hour. Following primary antibody incubation, membranes were subjected to three 10 minute wash steps in 1x TBS-T, and incubated with horseradish peroxidase-conjugated anti-chicken secondary antibody (ab6753) for 30 minutes at room temperature. Five additional 10 minute washes were performed in 1x TBS-T, and proteins were visualized using Amersham ECL Plus Western Blotting Detection Reagents (GE Healthcare Biosciences, Piscataway, NJ).

Drug treatment

Adult male rats received intracerebroventricular (i.c.v.) injections of morphine (Sigma-Aldrich Co., St. Louis, MO) dissolved in 0.9% saline to a concentration of 10 mg/ml and administered at 1.0 μg/kg (n =5), 0.9% saline in a volume of 25 μl/kg (n = 5) or DAMGO (Tocris Bioscience, Ellsville, MO) at 5μg/kg body weight (n = 5). Rats were anesthetized with isoflurane (Abbott Laboratories, North Chicago, IL; 0.5–1.0%, in air) via a specialized nose cone affixed to the sterotaxic frame (Stoelting Corp., Wood Dale, IL) and placed in a stereotaxic apparatus for surgery. Micropipettes (Kwik-Fil, 1.2 mm outer diameter; World Precision Instruments, Inc., Sarasota, FL) with tip diameters of 20–25 μm were filled with saline, morphine or DAMGO. The tips of the micropipettes were placed at the following coordinates, 3.5 mm posterior from bregma, 1.4 mm medial/lateral, 3.7 mm ventral from the top of the skull. The stereotaxic coordinates of the injection sites were based on the rat brain atlas of Paxinos and Watson (Paxinos and Watson, 1986). Saline, morphine or DAMGO was injected using a Picospritzer (General Valve Corporation, Fairfield, NJ) at 24–26 psi and over a 10 min period. Pipettes were left at the site of injection for 5 min following drug or vehicle administration.

Thirty minutes following i.c.v. injections of saline, morphine or DAMGO, rats were euthanized. The time of euthanasia post-treatment was selected based on previous studies from our group. Using an in vitro technique in MOR expressing human embryonic kidney 293 cells a MOR/WLS complex was detected 1 hour following DAMGO treatment (Jin et al., 2010a). Moreover, another in vivo study using high resolution electron microscopy in rat brain showed significant MOR internalization 30 min following treatment with the opiate agonist, etorphine (Van Bockstaele and Commons, 2001). Finally, it is well known that agonist-induced trafficking and up-regulation may occur rapidly from seconds to minutes (Norgauer et al., 1991; Zigmond et al., 1982) and the time point of 30 minutes was considered to be optimal for detecting changes in trafficking patterns here.

Immuno-electron microscopy

Thirty minutes following injection, rats were deeply anesthetized with sodium pentobarbital (80 mg/kg; Ovation Pharmaceuticals, Inc., Deerfield, IL, USA) and transcardially perfused through the ascending aorta with 10 ml heparinized saline followed by 25 ml of 3.75% acrolein (Electron Microscopy Sciences, Fort Washington, PA, USA), and 50 ml of 2% formaldehyde in 0.1 M phosphate buffer (PB; pH 7.4). The brains were removed immediately after perfusion fixation, sectioned into 1–3 mm coronal slices and postfixed in the same fixative overnight at 4°C.

Forty micron-thick coronal sections through the rostrocaudal extent of the striatum (Paxinos and Watson 1986) were cut using a Vibratome (Technical Product International, St Louis, MO, USA) and rinsed extensively in 0.1 M PB and 0.1 M tris-buffered saline (TBS; pH 7.6). Sections were placed for 30 min in 1% sodium borohydride in 0.1 M PB to reduce amine-aldehyde compounds. The tissue sections were then incubated in 0.5% bovine serum albumin (BSA) in 0.1 M TBS for 30 min. Subsequently, sections were incubated in chicken anti-WLS antiserum (Gene-Tel Laboratories, Madison, WI) at 1:1000 in 0.1% BSA and 0.1M TBS. Incubation time was 15–18 hours in a rotary shaker at room temperature. Thorough rinses in 0.1 M TBS were conducted following each incubation procedure.

WLS was visualized using the immunogold-silver enhancement technique. Tissue sections were rinsed three times with 0.1 M TBS, followed by rinses with 0.1 M PB and 0.01 M phosphate buffered saline (PBS; pH 7.4). This was followed by 10-minute incubation in a 0.2% gelatin-PBS and 0.8% BSA buffer and a two-hour incubation in goat anti-rabbit IgG conjugate in 1 nm gold particles (Amersham Bioscience Corp., Piscataway, NJ) at room temperature. Sections were then rinsed in buffer containing the same concentration of gelatin and BSA as above. Following rinses with 0.01 M PBS, sections were then incubated in 2% glutaraldehyde (Electron Microscopy Sciences) in 0.01 M PBS for 10 min. The conjugated gold particles were intensified by incubation in a silver enhancement solution (Amersham Bioscience Corp.). The optimal times for silver enhancement were determined by empirical observation for each experiment and ranged between 8 and 10 min. Following intensification, tissue sections were rinsed in 0.2 M citrate buffer and 0.1 M PB, and fixed in 2% osmium tetroxide (Electron Microscopy Sciences) in 0.1 M PB for 1 h, washed in 0.1 M PB, dehydrated in an ascending series of ethanol followed by propylene oxide and flat embedded in Epon 812 (Electron Microscopy Sciences; Leranth and Pickel, 1989) between tow sheets of Aclar plastic (Honeywell, Pottsville, PA).

Thin sections of approximately 50–100 nm in thickness were cut with a diamond knife (Diatome-US, Fort Washington, PA) using a Leica Ultracut (Leica Microsystems, Wetzlar, Germany). Captured images of selected sections were compared with captured light microscopic images of the block face before sectioning. Sections were collected on copper mesh grids, examined with an electron microscope (Morgagni, Fei Company, Hillsboro, OR) and digital images were captured using the AMT advantage HR/HR-B CCD camera

system (Advance Microscopy Techniques Corp., Danvers, MA, USA). Figures were assembled and adjusted for brightness and contrast in Adobe Photoshop CS4 software (Adobe Systems, Inc., San Jose, CA).

Immunogold-silver labeling for WLS appeared as intense black electron-dense particles and was identified in striatal somata and dendritic processes as we have recently demonstrated (Jin et al., 2010a; Reyes et al., 2010). Selective immunogold-silver labeled profiles were identified by the presence, in single thin sections, of at least two immunogold-silver particles within a cellular compartment (Jin et al., 2010a; Reyes et al., 2010). The criterion of two gold particles as indicative of WLS labeling is conservative and may have led to an underestimation of the number of WLS-labeled profiles. Another factor that may have led to the underestimation of labeled profiles is the limitation of immunocytochemical methods to detect trace amounts of WLS. To circumvent the caveat of incomplete antibody penetration which is inherent to preembedding technique, tissue sections were collected close to the plastic-tissue interface and to ensure that the immunogold labeling was detectable in all sections analyzed. Additionally, unbiased stereological methods were not used for counting labeled profiles, and the results of the numerical analysis can only be considered to be an estimate of the numbers of synapses and labeled profiles.

Sequential immunogold-silver labeling

Following the procedure for dual immunogold-silver labeling that we recently described in another study (Jin et al., 2010), WLS and MOR were identified using sequential immunogold-silver labeling. Tissue sections were incubated for 15–18 hours in a cocktail containing chicken anti-WLS antiserum (Gene-Tel Laboratories, Madison, WI) at 1:1000 and rabbit anti-MOR (Immunostar Inc., Hudson, WI, USA) at 1:2000 in 0.1%BSA and 0.1M TBS. Thereafter, sections were rinsed extensively in 0.1 M TBS and 0.2% BSA in 0.01 M PBS followed by incubation in goat anti-rabbit IgG ultra-small conjugate (1:100; Amersham Bioscience Corp., Piscataway, NJ, USA) at room temperature for 8 hours. Tissue sections were rinsed six times in 0.2% BSA-0.01 M PBS and twice in 0.1 M PB. Pre-enhancement washings were done with Enhancement Conditioning Solution (ECS; Amersham Bioscience Corp.) followed with the first silver enhancement (300 μl R-Gent SE-EM enhancement mixture; Amersham Bioscience Corp.) for 90 min. Subsequently, tissue sections were rinsed in 0.2 M citrate buffer, four times in ECS and two times in 0.1 M PB and were incubated in goat anti-chicken IgG ultra-small conjugate (1:100; Amersham Bioscience Corp.) at room temperature for 8 hours followed by rinses with 0.2% BSA-0.01 M PBS and 0.1 M PB. Then, sections were incubated in 2.5% glutaraldehyde (Electron Microscopy Sciences) in 0.01 M PBS for 2 hours followed by extensive rinses with 0.1 M PB and distilled water. The second silver enhancement (300 μl R-Gent SE-EM enhancement mixture; Amersham Bioscience Corp.) was performed for 60 min. Tissues sections were washed extensively with distilled water and 0.1 M PB. All washes were done at 10 min-intervals. Following washes, tissue sections were incubated in 2% osmium tetroxide (Electron Microscopy Sciences) in 0.1 M PB for 1 h, washed in 0.1 M PB, dehydrated in an ascending series of ethanol followed by propylene oxide and flat embedded in Epon 812. Sectioning with a diamond knife, examining with an electron microscope and obtaining digital images followed standard protocols described earlier.

Control and data analysis

Every fourth adjacent section through the striatum was included in immunohistochemical staining for WLS. Some sections were processed in parallel with the rest of the procedures identical but the primary antiserum was omitted. Sections processed in the absence of primary antibody did not exhibit immunoreactivity. (Jin et al., 2010a; Reyes et al., 2010). Tissue sections were taken from three rats per group with the good preservation of

ultrastructural morphology and with clearly apparent immunocytochemical labeling. At least 9 grids containing 5 to 8 thin sections each were collected from at least two plastic-embedded sections of the LC from each animal. The quantification of WLS-immunolabeled profiles were carried out at the plastic-tissue interface to ensure that immunolabeling was detectable in all sections used for analysis (Chan et al., 1990). To determine whether levels of spurious silver grains could contribute to false positives, blood vessels and myelinated axons (structures that should not contain WLS immunolabeling) were counted in random ultrathin sections. Minimal spurious labeling was identified. Therefore, the criteria for considering a process as immunolabeled was defined by the presence of at least 2–3 silver grains in a cellular profile. Only tissue sections that were singly labeled for WLS were used for the electron microscopic analysis. The identification of cellular elements was based on the standard morphological criteria (Peters et al., 1991; Peters and Palay, 1996). WLS immunolabeling was identified as either cytoplasmic or plasmalemmal. If the immunogold-silver grains were associated with the plasma membrane they were classified as plasmalemmal and if the immunogold-silver grains were not in contact with the plasma membrane they were classified as cytoplasmic. A total of 1279 dendritic profiles exhibiting WLS immunoreactivity from all groups were used in the analysis. Specifically, the dendritic profiles were randomly obtained from each rat and ranged in number from 119–182 dendritic profiles per animal. Statistical analysis of the number of profiles obtained showed no significant difference in the number of dendritic profiles sampled per group (saline = 121.67 ± 12.3; morphine 141.67 ± 31.78; DAMGO = 163 ± 17.06) examined between groups. The analysis of WLS internalization in various groups studied was quantified by calculating the ratio of cytoplasmic to total immunogold-silver particles for each singly immunolabeled dendritic profile in individual rats. The density of WLS on the plasma membrane was calculated as the number of plasmalemmal immunogold-silver particles per unit perimeter (μm). Similarly, the density of WLS in the cytoplasm was calculated as the number of cytoplasmic immunogold-silver particles per unit area (μm^2). All the data gathered and analyzed were obtained per animal and the average of three animals was calculated. The perimeter and area of each dendritic profle was obtained using Image J software (NIH). In addition, as with previous studies from our group (Reyes et al., 2006; Reyes et al., 2008; Wang et al., 2009), care was taken to ensure that control and experimental groups contained similarly sized profiles. We did not observe any statistical difference in the size of profiles analyzed in any group examined as we have recently reported (Reyes et al., 2010). For the sequential immunogold-silver labeling, semi-quantitative analysis was carried out by randomly obtaining the ratio of cytoplasmic to total immunogold-silver particles for WLS and MOR in a dendritic profile exhibiting both WLS and MOR immunoreactivities.

Results

WLS shifts its distribution following opiate agonist treatment

Consistent with our recent reports (Jin et al., 2010a; Reyes et al., 2010), WLS immunoreactivity was distributed within somata and dendritic processes in the rat striatum. Using immunoelectron microscopy, WLS was labeled using immunogold-silver detection where immunolabeling appeared as irregularly shaped black deposits indicative of the antigen of interest (Figure 1A–H). The localization of WLS, in the present study, supports our recent description provided in a mouse model (Reyes et al., 2010).

Using immunoelectron microscopy, we examined the distribution of WLS in striatal dendrites following exposure to morphine and DAMGO, and compared this to vehicle-treated subjects. We recently reported that the ratio of cytoplasmic to total immunogold-silver particles as well as the number of immunogold-silver particles per micron of plasmalemma and the number of immunogold-silver particles per micron square did not

significantly differ between large- (>5 μm in perimeter) and small- (<5 μm in perimeter) sized dendrites when examining the localization of WLS (Reyes et al., 2010). Therefore, in the present study, we pooled the data collected from large and small dendrites.

Rats injected with saline showed immunogold-silver particles indicative of WLS along the plasma membrane and within the cytoplasm of striatal dendrites (Figure 1A–B). Conversely, in morphine-treated rats, WLS immunogold-silver particles were localized along the plasma membrane of striatal dendrites (Figure 1C–D). Interestingly, when rats were injected with DAMGO, immunogold-silver particles indicative of WLS were localized primarily within the cytoplasmic compartment (Figure 1E–F). Semi-quantitative ultrastructural analysis revealed in Figure 2 that the density of WLS-immunogold silver particles per micron was significantly higher along the plasmalemma of morphine-treated rats compared to saline- and DAMGO-treated rats ($F_{2,6} = 9.68$; $P < 0.0132$). Furthermore, the density of WLS-immunogold silver particles per micron square (Figure 2; $F_{2,12} = 46.57$; $P < 0.0003$) and the ratio of cytoplasmic to total WLS-silver grains (Figure 3; $F_{2,12} = 90.69$; $P < 0.0001$) were significantly lower in morphine-treated rats compared to saline- and DAMGO-treated rats. Also, DAMGO-treated rats had a higher density of WLS-immunogold silver particles per micron square (Figure 2; $F_{2,12} = 46.57$; $P < 0.0003$) and ratio of cytoplasmic to total WLS-silver grains (Figure 3; $F_{2,12} = 90.69$; $P < 0.0001$) when compared to saline- and morphine-treated rats. Following morphine treatment, the total number of WLS-immunogold silver particles was significantly lower in the intracellular compartment compared to saline and DAMGO-treated rats (Table 1; $F_{2,12} = 28.43$; $P < 0.0001$). Following DAMGO treatment, the total number of WLS-immunogold silver particles was significantly higher in the cytoplasm compared to saline- and morphine-treated rats (Table 1; $F_{2,12} = 28.43$; $P < 0.0001$).

We also analyzed tissue sections that were dually labeled with immunogold-silver sequentially where the immunogold-silver particles were differentiated based on their size (Figure 4). Obtaining different sized immunogold-silver particles was achieved by incubating with one ultrasmall gold conjugate, followed by silver enhancement, and then incubating with the second ultrasmall gold conjugate, followed by additional silver enhancement (Yi et al., 2001). This resulted in two groups of silver-enhanced particles: smaller particles that were enhanced once and larger particles that were enhanced twice (Reyes et al., 2011; Jin et al., 2010A, Yi et al., 2001). Dual immunogold-silver labeling (large and small gold-silver particles, for MOR and WLS, respectively) were localized in the same tissue section (Figure 4). Gold-silver labeling for MOR and WLS were readily distinguishable from each other and were localized to the appropriate cellular structures (Figure 4). MOR-immunogold-silver particles appeared as large black punctate particles along the plasma membrane of dendrites while WLS-immunogold-silver particles appeared as smaller black punctate particles within the dendrites (Figure 4). Following saline and morphine treatment, MOR was consistently localized along the plasma membrane of striatal dendrites as previously described (Reyes et al., 2010). WLS in saline-treated rats showed a significant distribution within the cytoplasmic compartment of striatal dendrites; however following morphine treatment, there was a significant shift of distribution from the cytoplasm to the plasma membrane ($P < 0.05$) in MOR-containing profiles.

WLS-containing dendrites frequently receive synapses from axon terminals

In agreement with our recent report (Reyes et al., 2010), WLS-labeled dendrites received both symmetric and asymmetric-type synapses from unlabeled axon terminals. Of the three experimental groups examined, a total of 1000 synapses contacting with WLS-labeled dendrites were analyzed. Of the total synapses examined, 61% (608/1000) received defined synaptic specializations while 39% (392/1000) received synaptic specializations from unlabeled axon terminals that were difficult to unequivocally establish due to the plane of

section analyzed. Of the 608 WLS-labeled dendrites with identifiable synapses, 43% (426/1000) received symmetric (inhibitory-type) synapses while 18% (182/1000) received asymmetric (excitatory-type) synapses. Statistical analysis showed that there was no significant difference observed between the groups studied with respect to the kind of synapses contacting with WLS-labeled dendrites (Figure 5).

Discussion

This study provides the first *in vivo* evidence of opiate agonist-induced trafficking of WLS that is consistent with data obtained using *in vitro* systems (Jin et al, 2010a). Here, we show that following morphine treatment, WLS is more frequently distributed along the plasma membrane when compared to saline-treated rats. Interestingly, following DAMGO treatment, WLS was more often distributed within the cytoplasm. These data suggest that opiate agonists induce differential trafficking of WLS in the striatum.

Technical considerations

WLS was localized using a high resolution pre-embedding immunogold detection method. This technique provides superior subcellular localization of the antigen of interest while preserving optimal ultrastructural morphology (Leranth and Pickel, 1989). The pre-embedding method is more appropriate than the postembedding method for localization of immunoreactivity at extrasynaptic sites making quantification of WLS distribution more suitable (Lujan et al., 1996).

Immunolabeling in thick sections prior to embedding can produce limited reagent penetration and is a caveat with this approach. In order to minimize issues of penetration 1) we collected tissue sections near the tissue-Epon interface where penetration of the antibody is optimal to ensure that immunolabeling was clearly detectable in sections included in the analysis (Chan et al., 1990), 2) profiles were sampled only when immunoreactivity was clearly present in sections included in the analysis, 3) sections were processed in parallel to facilitate relative comparisons (Reyes et al., 2010), and a comparable number of dendritic profiles for each experimental animal was analyzed so that any limitation of the preembedding technique would not contribute to group differences.

Another consideration in the interpretation of these results includes specificity of antisera used. The WLS antibody was raised in chicken against a peptide antigen corresponding to the C-terminal 18 amino acids (HVDGPTEIYKLTRKEAQE) of human WLS (Gene-Tel Laboratories, Madison, WI) which is identical to the rat and mouse peptide sequence. A polyclonal antibody, WLS of IgY subtype was harvested from yolk and affinity-purified prior to use (Jin et al., 2010a; Jin et al., 2010B). The characterization and specifity of the chicken antiserum against WLS has been previously described (Jin et al. 2010a,b). The specificity of WLS was ascertained by transfecting a FLAG/6x His-tagged WLS cDNA into HEK293 cells. Using western blot analysis WLS immunoreactivity was expressed in lysates prepared from transfected cells which were first probed with anti-FLAG antibody, then stripped and reprobed with anti WLS antibody. A band migrating with the identical molecular mass was detected with anti-FLAG and anti-WLS antibodies indicating that WLS antibody was specific for the WLS protein. In transfected cells, WLS recognized a single protein species with an approximate molecular weight of about 50 kDa (Jin et al., 2010a). In the present study, preabsorption of WLS with antigenic peptide blocked the WLS immunoreactivity in the frontal cortex (Figure 1B′).

The potential effect of exposure to the anesthetic (used for drug delivery) or internalization of receptors warrants some discussion. Studies using primary cortical cell cultures exposed to propofol and adult male mouse cortical neurons administered i.p. with chloral hydrate

suggest that exposure to anesthetics may influence internalization of receptors (LacKamp et al., 2009; Oscarsson et al., 2010). However, Oscarsson and colleague used a cell culture system suggesting that differences in internalization may exist depending on the experimental model used (Oscarsson et al., 2010). Morever, the use of different anesthetics may influence internalization patterns depending on the time point analyzed (LacKamp et al., 2009). Importantly, we did not see similar patterns of trafficking in vehicle-treated rats that had undergone similar anesthesia exposure suggesting that the use of anesthetics in our study did not confound the analysis.

Opiate agonists induce trafficking of WLS in striatal neurons

Using protein sequence analysis, WLS shows a high percentage of identity in vertebrate species (Fu et al., 2009). As such, human WLS is 96% identical to mouse WLS and 78% identical to zebrafish protein. The C-terminal peptide used to generate the anti-WLS antibody showed a high degree of sequence conservation so that this segment of human, mouse and rat WLS is 100% identical while the human and zebrafish proteins differ at only 2 of 18 residues of this domain (Jin et al. 2010b). Furthermore, western blot analysis indicated that anti-human WLS antibodies are specific for WLS and immunoreact with endogenous WLS from a variety of mammalian species (Jin et al., 2010b). We have recently reported the distribution of WLS in striatal somata and in dendritic processes in mouse brain tissue sections using immunofluorescence and immunoelectron microscopy (Jin et al., 2010a, Reyes et al., 2010). Using rat brain tissue, we extended our previous results by showing that WLS is localized in the somata and in dendritic processes of rat striatal neurons. Using Western blot analysis and in-situ hybridization, WLS has also been shown to be localized in several other brain regions including cortex, hippocampus, ventral tegmentum, nucleus accumbens and cerebellum (Jin et al., 2010b). Likewise, WLS was also expressed in peripheral tissues, including skeletal muscle, heart muscle, lung, gut, liver and kidney (Jin et al., 2010b). The widespread distribution and expression of WLS may suggest that WLS plays an essential role in regulating Wnt secretion throughout the body.

WLS has a transmembrane structure similar to that of a G-protein coupled receptor (GPCR) (Fu et al., 2009) and functionally interacts with the MOR (Jin et al., 2010a, 2010b). It has been proposed that WLS contains four (Goodman et al., 2006), seven (Banziger et al., 2006) or eight (Bartscherer et al., 2006) membrane spanning domains. All of these models predict that the WLS membrane-spanning domains contain an N-terminal signal sequence. Two potential N-linked glycosylation sites in human WLS sequence at residues N8 and N306 have been recently identified (Jin et al., 2010b). The N terminus of WLS is likely to be intracellular, and residue N8 is predicted to be located in the cytosol. Likewise, N406 is predicted to be located in the cytoplasmic compartment in all three models of the WLS structure (Jin et al., 2010b). *In vitro* studies using HEK 293 cells stably expressing FLAG-tagged MORs (293-MOR cells) and transiently transfected with a FLAG/6x His-tagged WLS construct showed that morphine treatment induced an increased co-localization of MOR and WLS where WLS was predominantly localized along the periphery (Jin et al., 2010a). Conversely, following DAMGO treatment, WLS was distributed within the cytosolic compartment where it was co-localized with MOR (Jin et al., 2010a).

Our present study also shows that WLS-containing dendrites in striatal neurons frequently receive synapses from unlabeled axon terminals. The unlabeled axon terminals formed either symmetric, asymmetric or “undefined” synapses. The undefined synapses refer to synaptic specializations that were difficult to unequivocally establish due to the plane of tissue analyzed. We have recently shown that WLS and MOR-labeled dendrites were targeted by axon terminals that form symmetric synapse (Reyes et al., 2010). In our findings we consistently showed a preponderance of symmetric synapses that target WLS-containing dendrites. Symmetric synapses have been correlated with inhibitory transmission whereas

asymmetric synapses have been correlated with excitatory transmission (Gray, 1959; Carlin et al., 1980; Carlin et al., 1981; Peters et al., 1991; Peters & Palay, 1996). Anatomically, it has been shown that enkephalin (ENK)-containing neurons are localized in striatal neurons (Pickel et al., 1992). Additionally, we have recently shown that WLS and MOR-containing striatal neurons are enkephalinergic (Reyes et al., 2010). Furthermore, the striatum is enriched with GABA-containing neurons (Graveland and DiFiglia, 1985; Gerfen and Wilson, 1996) and these GABAergic neurons serve as primary source of synaptic inhibition in the striatum (Koos et al., 2004; Taverna et al., 2007). Taken together, it is likely that unlabeled axon terminals targeting WLS-containing dendrites may represent inhibitory (ENK or GABA) axon terminals that may hyperpolarize striatal neuronal activity. However, whether the WLS-containing neurons following opioid treatment contain either ENK, GABA or both requires further investigation.

Functional implications

The MOR/WLS interaction may play a role in agonist-induced re-distribution of WLS which is differentially influenced by opiate agonists. As binding partners, interactions between MOR and WLS may occur in the cytosolic compartment or the plasma membrane of cells (Jin et al., 2010a). Such associations have implications for receptor function. Johnson and colleagues reported that morphine-desensitized receptors are not internalized but are retained on the plasma membrane in the desensitized form as a result of different conformational changes of MORs being stabilized by different agonists that recruit different regulatory elements to the receptor (Johnson et al., 2006). Specifically, it was suggested that desensitization and tolerance to morphine are mediated largely by protein kinase C while desensitization by DAMGO is mediated by a G protein-coupled receptor kinase (Bailey et al., 2004; Johnson et al., 2006). We hypothesize that when morphine binds with MOR, the morphine-enhanced interaction between MOR and WLS causes entrapment of WLS at the cell surface and WLS is inefficiently internalized (Figure 6). As a result, a larger proportion of MOR and WLS is present at the plasma membrane enabling more MOR to be available for activation by morphine (Figure 6). This event effectively sequesters WLS, thereby inhibiting WLS function in mediating Wnt secretion since a significant inhibition of Wnt secretion was observed in morphine-treated 293-MOR cells (Jin et al., 2010a). While WLS is inefficiently internalized after morphine, WLS is efficiently internalized in the presence of DAMGO (Figure 6; Jin et al., 2010a).

MORs show ligand-dependent mechanism of desensitization and internalization (Arttamangkul et al., 2008; Johnson et al., 2006). A differential desensitization and internalization of MOR has been extensively described depending on the agonist involved (Bailey et al., 2003; Johnson et al., 2006). Specifically, DAMGO treatment results in arrestin-2 translocation to the plasma membrane with MOR desensitization and significant internalization (Bailey et al., 2003; Johnson et al., 2006; McPherson et al., 2010, Haberstock-Debic et al., 2005). Nevertheless, the ability of morphine to induce desensitization and internalization has been debated (McPherson et al., 2010, Haberstock-Debic et al., 2005). While some groups report that morphine does not induce arrestin-2 translocation and induces very little MOR internalization (Bailey et al., 2003, Johnson et al., 2006), other studies report otherwise (McPherson et al., 2010, Haberstock-Debic et al., 2005). The discrepancy between these findings may be related to differences in model systems employed. In addition, different agonists can activate distinct MOR signaling pathways beyond differences in internalization (Whistler et al., 1999; Melief et al., 2010).

An interaction between WLS and Wnt proteins has been demonstrated in the Golgi complex and these two proteins shuttle together to the plasma membrane where Wnt proteins are then released (Banziger et al., 2006). It is via a clathrin-mediated endocytosis that WLS is internalized, while it is via the retromer complex that WLS is recycled back to the Golgi

(Franch-Marro et al., 2008, Port et al., 2008). WLS binds with MOR and their association occurs both in the cytoplasmic compartment as well as on the plasma membrane (Jin et al. 2010a). Following morphine treatment, the level of MOR/WLS complexes significantly increased using immunoprecipitation and immunohistochemistry (Jin et al., 2010a). Consistent with our previous report (Jin et al., 2010a), our present results show that following morphine treatment, WLS is redistributed from the cytoplasmic compartment to the plasma membrane. It is likely that following morphine treatment, MORs are inefficiently internalized as we (Van Bockstaele and Commons, 2001) and others (Keith et al., 1996) have previously reported. This event then leads to an increase in the association between WLS and MOR that may potentially cause WLS to be translocated to the plasma membrane and effectively sequestered there. In turn, WLS recycling is reduced thereby inhibiting Wnt secretion. It is tempting to speculate that the WLS trafficking reported here occurs in MOR-containing dendrites. We have recently demonstrated an interaction between the MOR and WLS at the ultrastructural level in the striatum (Reyes et al., 2010). Specifically, somata and dendritic processes exhibiting WLS, also contained MOR (Reyes et al., 2010). However, further studies are required to address the specific phenotype of neurons where WLS trafficking is induced by MOR agonist administration.

The present observations of differential trafficking of WLS have implications for actions of opiate drugs in the central nervous system. It is known (Robinson and Kolb, 1999, Eisch et al., 2000) that even after a few days of chronic morphine exposure, a widespread loss of dendritic spines has been observed (Liao et al, 2007). Wnt proteins have been known to play a significant role in morphological patterning during development (Wodarz and Nusse, 1998), in stem cell maintenance (Toledo et al., 1998), cancer (Reya and Clevers, 2005), neuronal development (Salinas and Zou, 2008) and synaptic remodeling (Speese and Budnik, 2007). Wnt proteins are required for maintenance of dendritic spines. If morphine causes increased WLS-MOR interaction, rendering WLS unable to secrete Wnt proteins, loss of dendritic spines might ensue, secondary to a dearth of Wnt proteins. If loss of dendritic spines contributes to the cognitive deficits seen after chronic opioid agonist use (Sjogren et al, 2000), then inhibiting the WLS-MOR interaction might prevent the loss of spines and the subsequent cognitive deficits.

Exposure to chronic morphine also causes decreased neurogenesis in hippocampus (Eisch et al,, 2000). Wnts are essential to the process of hippocampal neurogenesis (Lie et al., 2005). MOR-WLS dimerization and sequestration at the plasma membrane after morphine may represent the mechanism whereby morphine causes decreased hippocampal neurogenesis.

It is tempting to speculate that following DAMGO treatment, MOR/WLS complexes are internalized, which is accompanied by disassociation of these complexes so that WLS is recycled to the Golgi through the retromer complex. While in the Golgi, WLS is able to associate with Wnt proteins that are then translocated back to the plasma membrane for release (Banziger et al., 2006). This could partly explain the unchanged Wnt secretion following DAMGO treatment (Jin et al., 2010a).

In summary, using high resolution electron microscopy, we provide the first *in vivo* evidence that exposure to opiate agonist causes a redistribution of WLS in rat striatal neurons. The differential redistribution of WLS may partly underlie the opioid-induced dysregulation in Wnt secretion that may lead to morphological and physiological alterations in striatal neurons.

Acknowledgments

Grant information: This project was supported by the National Institutes of Health grant P20 DA #025995 and DA #05186 to W.H.B. and DA #09082 to E.V.B.

This project was supported by the National Institutes of Health grants P20 DA 025995 and DA 05186 to W.H.B. and DA 09082 to E.V.B.

References

Arttamangkul S, Quillinan N, Low MJ, von Zastrow M, Pintar J, Williams JT. Differential activation and trafficking of micro-opioid receptors in brain slices. Mol Pharmacol. 2008; 74:972–979. [PubMed: 18612077]

Bailey CP, Connor M. Opioids: cellular mechanisms of tolerance and physical dependence. Curr Opin Pharmacol. 2005; 5:60–68. [PubMed: 15661627]

Bailey CP, Couch D, Johnson E, Griffiths K, Kelly E, Henderson G. Mu-opioid receptor desensitization in mature rat neurons: lack of interaction between DAMGO and morphine. J Neurosci. 2003; 23:10515–10520. [PubMed: 14627635]

Bailey CP, Kelly E, Henderson G. Protein kinase C activation enhances morphine-induced rapid desensitization of mu-opioid receptors in mature rat locus ceruleus neurons. Mol Pharmacol. 2004; 66:1592–1598. [PubMed: 15361548]

Banziger C, Soldini D, Schutt C, Zipperlen P, Hausmann G, Basler K. Wntless, a conserved membrane protein dedicated to the secretion of Wnt proteins from signaling cells. Cell. 2006; 125:509–522. [PubMed: 16678095]

Bartscherer K, Pelte N, Ingelfinger D, Boutros M. Secretion of Wnt ligands requires Evi, a conserved transmembrane protein. Cell. 2006; 125:523–533. [PubMed: 16678096]

Carlin RK, Grab DJ, Cohen RS, Siekevitz P. Isolation and characterization of postsynaptic densities from various brain regions: enrichment of different types of postsynaptic densities. J Cell Biol. 1980; 86:831–845. [PubMed: 7410481]

Carlin RK, Grab DJ, Siekevitz P. Function of a calmodulin in postsynaptic densities. III Calmodulin-binding proteins of the postsynaptic density. J Cell Biol. 1981; 89:449–455. [PubMed: 6265467]

Chan J, Aoki C, Pickel VM. Optimization of differential immunogold-silver and peroxidase labeling with maintenance of ultrastructure in brain sections before plastic embedding. J Neurosci Methods. 1990; 33:113–127. [PubMed: 1977960]

Ciani L, Salinas PC. WNTs in the vertebrate nervous system: from patterning to neuronal connectivity. Nat Rev Neurosci. 2005; 6:351–362. [PubMed: 15832199]

Clevers H. Wnt/beta-catenin signaling in development and disease. Cell. 2006; 127:469–480. [PubMed: 17081971]

Eisch AJ, Barrot M, Schad CA, Self DW, Nestler EJ. Opiates inhibit neurogenesis in the adult rat hippocampus. Proc Natl Acad Sci USA. 2000; 97:7579–7584. [PubMed: 10840056]

Franch-Marro X, Wendler F, Guidato S, Griffith J, Baena-Lopez A, Itasaki N, Maurice MM, Vincent JP. Wingless secretion requires endosome-to-Golgi retrieval of Wntless/Evi/Sprinter by the retromer complex. Nat Cell Biol. 2008; 10:170–177. [PubMed: 18193037]

Fu J, Jiang M, Mirando AJ, Yu HM, Hsu W. Reciprocal regulation of Wnt and Gpr177/mouse Wntless is required for embryonic axis formation. Proc Natl Acad Sci USA. 2009; 106:18598–18603. [PubMed: 19841259]

Goodman RM, Thombre S, Firtina Z, Gray D, Betts D, Roebuck J, Spana EP, Selva EM. Sprinter: a novel transmembrane protein required for Wg secretion and signaling. Development. 2006; 133:4901–4911. [PubMed: 17108000]

Gray EG. Axosomatic and axo-dendritic synapses of the cerebral cortex: an electron microscopic study. J Anat. 1959; 93:420–433. [PubMed: 13829103]

Gerfen, CR.; Wilson, CJ. The basal ganglia. In: Swanson, LW.; Bjorklund, A.; Hokfelt, T.; Heimer, L.; Zaborszky, L., editors. Handbook of chemical neuroanatomy. Vol. 12. Amsterdam: Elsevier Science; 1996. p. 371-468.

Graveland GA, DiFiglia M. The frequency and distribution of medium-sized neurons with indented nuclei in the primate and rodent neostriatum. Brain Res. 1985; 327:307–311. [PubMed: 3986508]

Grigoryan T, Wend P, Klaus A, Birchmeier W. Deciphering the function of canonical Wnt signals in development and disease: conditional loss- and gain-of-function mutations of beta-catenin in mice. Genes Dev. 2008; 22:2308–2341. [PubMed: 18765787]

Haberstock-Debic H, Kim KA, Yu YJ, von Zastrow M. Morphine promotes rapid, arrestin-dependent endocytosis of mu-opioid receptors in striatal neurons. J Neurosci. 2005; 25:7847–7857. [PubMed: 16120787]

Hull LC, Llorente J, Gabra BH, Smith FL, Kelly E, Bailey C, Henderson G, Dewey WL. The effect of protein kinase C and G protein-coupled receptor kinase inhibition on tolerance induced by mu-opioid agonists of different efficacy. J Pharmacol Exp Ther. 2010; 332:1127–1135. [PubMed: 20008489]

Jin J, Kittanakom S, Wong V, Reyes BAS, Van Bockstaele EJ, Stagljar I, Berrettini W, Levenson R. Interaction of the mu-opioid receptor with GPR177 (Wntless) inhibits Wnt secretion: potential implications for opioid dependence. BMC Neurosci. 2010a; 11:33. [PubMed: 20214800]

Jin J, Morse M, Frey C, Petko J, Levenson R. Expression of GPR177 (Wntless/Evi/Sprinter), a highly conserved Wnt-transport protein, in rat tissues, zebrafish embryos, and cultured human cells. Dev Dyn. 2010b; 239:2426–2434. [PubMed: 20652957]

Johnson EA, Oldfield S, Braksator E, Gonzalez-Cuello A, Couch D, Hall KJ, Mundell SJ, Bailey CP, Kelly E, Henderson G. Agonist-selective mechanisms of mu-opioid receptor desensitization in human embryonic kidney 293 cells. Mol Pharmacol. 2006; 70:676–685. [PubMed: 16682505]

Kehagia AA, Murray GK, Robbins TW. Learning and cognitive flexibility: frontostriatal function and monoaminergic modulation. Curr Opin Neurobiol. 2010; 20:199–204. [PubMed: 20167474]

Keith DE, Murray SR, Zaki PA, Chu PC, Lissin DV, Kang L, Evans CJ, von Zastrow M. Morphine activates opioid receptors without causing their rapid internalization. J Biol Chem. 1996; 271:19021–19024. [PubMed: 8702570]

Koos T, Tepper JM, Wilson CJ. Comparison of IPSCs evoked by spiny and fast-spiking neurons in the neostriatum. J Neurosci. 2004; 24:7916–7922. [PubMed: 15356204]

LacKamp A, Zhang GC, Mao LM, Fibuch EE, Wang JQ. Loss of surface N-methyl-D-aspartate receptor proteins in mouse cortical neurones during anaesthesia induced by chloral hydrate in vivo. Br J Anaesth. 2009; 102:515–522. [PubMed: 19224925]

Leranth, C.; Pickel, VM. Electron microscopic preembedding double-labeling methods. In: Heimer, L.; Zaborszky, L., editors. Neuroanatomical tracing methods. 1. Vol. 2. New York: Plenum Press; 1989. p. 129-172.

Liao D, Grigoriants OO, Wang W, Wiens K, Loh HH, Law PY. Distinct effects of individual opioids on the morphology of spines depend upon the internalization of mu opioid receptors. Mol Cell Neurosci. 2007; 35:456–69. [PubMed: 17513124]

Lie DC, Colamarino SA, Song HJ, Desire L, Mira H, Consiglio A, Lein ES, Jessberger S, Lansford H, Dearie AR, Gage FH. Wnt signalling regulates adult hippocampal neurogenesis. Nature. 2005; 437:1370–1375. [PubMed: 16251967]

Logan CY, Nusse R. The Wnt signaling pathway in development and disease. Annu Rev Cell Dev Biol. 2004; 20:781–810. [PubMed: 15473860]

Lujan R, Nusser Z, Roberts JD, Shigemoto R, Somogyi P. Perisynaptic location of metabotropic glutamate receptors mGluR1 and mGluR5 on dendrites and dendritic spines in the rat hippocampus. Eur J Neurosci. 1996; 8:1488–1500. [PubMed: 8758956]

McPherson J, Rivero G, Baptist M, Llorente J, Al-Sabah S, Krasel C, Dewey WL, Bailey CP, Rosethorne EM, Charlton SJ, Henderson G, Kelly E. mu-opioid receptors: correlation of agonist efficacy for signalling with ability to activate internalization. Mol Pharmacol. 2010; 78:756–766. [PubMed: 20647394]

Melief EJ, Miyatake M, Bruchas MR, Chavkin C. Ligand-directed c-Jun N-terminal kinase activation disrupts opioid receptor signaling. Proc Natl Acad Sci USA. 2010; 107:11608–11613. [PubMed: 20534436]

Milligan G. Opioid receptors and their interacting proteins. Neuromolecular Med. 2005; 7:51–59. [PubMed: 16052038]

Norgauer J, Eberle M, Fay SP, Lemke HD, Sklar LA. Kinetics of N-formyl peptide receptor up-regulation during stimulation in human neutrophils. J Immunol. 1991; 146:975–980. [PubMed: 1988505]

Oscarsson A, Juhas M, Sjolander A, Eintrei C. The effect of propofol on actin, ERK-1/2 and GABAA receptor content in neurones. Acta Anaesthesiol Scand. 2007; 51:1184–1189. [PubMed: 17850559]

Paxinos, G.; Watson, C. The rat brain in stereotaxic coordinates. New York: Academic Press; 1986.

Peters A, Palay SL. The morphology of synapses. J Neurocytol. 1996; 25:687–700. [PubMed: 9023718]

Peters, A.; Palay, SL.; Webster, Hd. The Fine Structure of the Nervous System. New York: Oxford University Press; 1991.

Pickel VM, Chan J, Sesack SR. Cellular basis for interactions between catecholaminergic afferents and neurons containing Leu-enkephalin-like immunoreactivity in rat caudate-putamen nuclei. J Neurosci Res. 1992; 31:212–230. [PubMed: 1349353]

Port F, Kuster M, Herr P, Furger E, Banziger C, Hausmann G, Basler K. Wingless secretion promotes and requires retromer-dependent cycling of Wntless. Nat Cell Biol. 2008; 10:178–185. [PubMed: 18193032]

Reya T, Clevers H. Wnt signalling in stem cells and cancer. Nature. 2005; 434:843–850. [PubMed: 15829953]

Reyes AR, Levenson R, Berrettini W, Van Bockstaele EJ. Ultrastructural relationship between the mu opioid receptor and its interacting protein, GPR177, in striatal neurons. Brain Res. 2010; 1358:71–80. [PubMed: 20813097]

Reyes B, AS, Chavkin C, Van Bockstaele EJ. Agonist-induced internalization of kappa-opioid receptors in noradrenergic neurons of the rat locus coeruleus. J Chem Neuroanat. 2010; 40:301–309. [PubMed: 20884346]

Reyes BAS, Fox K, Valentino RJ, Van Bockstaele EJ. Agonist-induced internalization of corticotropin-releasing factor receptors in noradrenergic neurons of the rat locus coeruleus. Eur J Neurosci. 2006; 23:2991–2998. [PubMed: 16819988]

Reyes BAS, Valentino RJ, Van Bockstaele EJ. Stress-induced intracellular trafficking of corticotropin-releasing factor receptors in rat locus coeruleus neurons. Endocrinology. 2008; 149:122–130. [PubMed: 17947354]

Robinson TE, Kolb B. Morphine alters the structure of neurons in the nucleus accumbens and neocortex of rats. Synapse. 1999; 33:160–162. [PubMed: 10400894]

Salinas PC, Zou Y. Wnt signaling in neural circuit assembly. Annu Rev Neurosci. 2008; 31:339–358. [PubMed: 18558859]

Sjogren P, Thomsen AB, Olsen AK. Impaired neuropsychological performance in chronic nonmalignant pain patients receiving long-term oral opioid therapy. J Pain Symptom Manage. 2000; 19:100–108. [PubMed: 10699537]

Speese SD, Budnik V. Wnts: up-and-coming at the synapse. Trends Neurosci. 2007; 30:268–275. [PubMed: 17467065]

Taverna S, Canciani B, Pennartz CM. Membrane properties and synaptic connectivity of fast-spiking interneurons in rat ventral striatum. Brain Res. 2007; 1152:49–56. [PubMed: 17459351]

Toledo EM, Colombres M, Inestrosa NC. Wnt signaling in neuroprotection and stem cell differentiation. Prog Neurobiol. 2008; 86:281–296. [PubMed: 18786602]

Van Bockstaele EJ, Commons KG. Internalization of mu-opioid receptors produced by etorphine in the rat locus coeruleus. Neuroscience. 2001; 108:467–477. [PubMed: 11738260]

Wang Y, Xu W, Huang P, Chavkin C, Van Bockstaele EJ, Liu-Chen LY. Effects of acute agonist treatment on subcellular distribution of kappa opioid receptor in rat spinal cord. J Neurosci Res. 2009; 87:1695–1702. [PubMed: 19130621]

Watson DJ, Stanton ME. Spatial discrimination reversal learning in weanling rats is impaired by striatal administration of an NMDA-receptor antagonist. Learn Mem. 2009; 16:64–572.

Wodarz A, Nusse R. Mechanisms of Wnt signaling in development. Annu Rev Cell Dev Biol. 1998; 14:59–88. [PubMed: 9891778]

Zigmond SH, Sullivan SJ, Lauffenburger DA. Kinetic analysis of chemotactic peptide receptor modulation. J Cell Biol. 1982; 92:34–43. [PubMed: 6276415]

Research Highlights

- Wntless (WLS) mediates Wnt protein secretion, critical for neuronal development.
- Morphine induced a shift of WLS from the cytoplasm to the plasma membrane.
- DAMGO treatment induced a greater distribution of WLS intracellularly.
- Agonist-induced trafficking of WLS in striatum is shown after agonist exposure.
- WLS trafficking may represent a novel target in the treatment of opiate addiction.

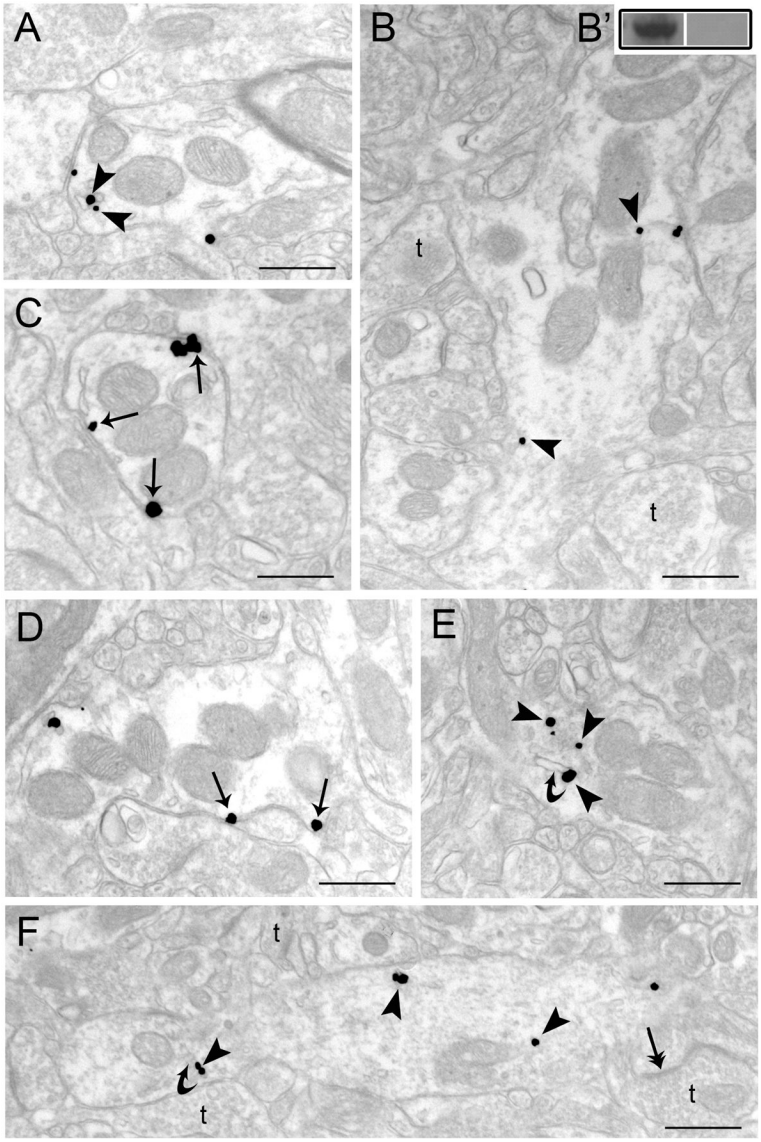

Figure 1.

Electron microscopic evidence for agonist-induced trafficking of WLS in rat striatum. Sections from control (vehicle-treated) (A, B), morphine-treated (C–D) and DAMGO-treated rats (E–F). **A–B.** Immunogold-silver labeling for WLS (arrowheads) can be seen in dendrites from vehicle-treated rats. **B′.** Western blot analysis showing WLS immunoreactivity in a frontal cortex microsample (left lane) and a preabsorption control using the immunizing protein (right lane). **C–D.** WLS labeling is more prominently distributed along the plasmalemma of striatal dendrites following morphine treatment. Arrows point to immunogold-silver labeling along the plasmalemma. **E–F.** Immunogold-silver labeling for WLS can be seen within the cytoplasm (arrowheads) in dendrites from a DAMGO-treated rat. Curved arrows point to endosome-like vesicles. Double headed arrows indicate synaptic specializations formed by axon terminals (t). Scale bars, 0.5μm.

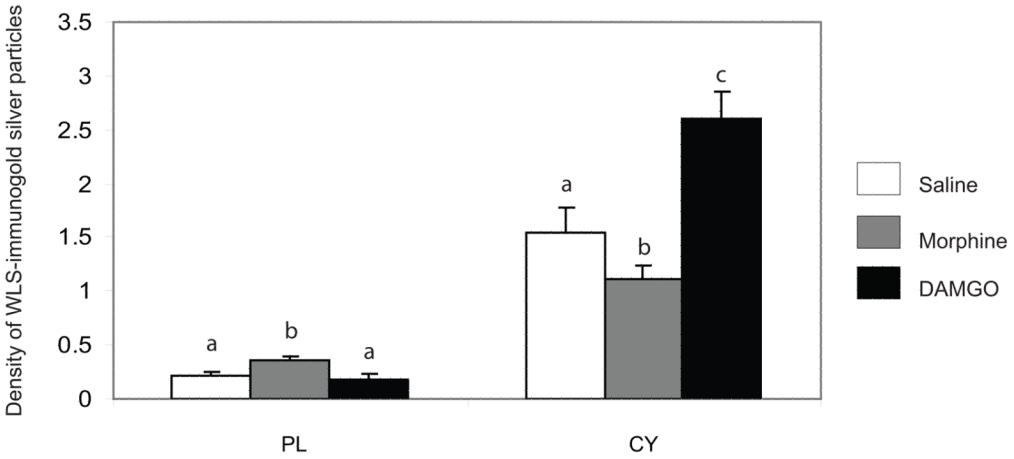

Figure 2.

The distribution of immunogold-silver particles indicative of WLS following opiate agonist treatment. The number of immunogold-silver particles following morphine treatment was significantly increased ($P<0.0001$) on the plasma membrane (PL) and decreased ($P<0.0001$) in the cytoplasm (CY) compared to saline- (control) and DAMGO-treated rats. The number of immunogold-silver particles following DAMGO treatment on the PL was comparable with control rats but was significantly increased ($P<0.0001$) in the CY compared to saline- (control) and morphine-treated rats. Values are means ± SEM of five rats per group. Values with different letters are significantly different from each other (Tukey's multiple comparison test after ANOVA).

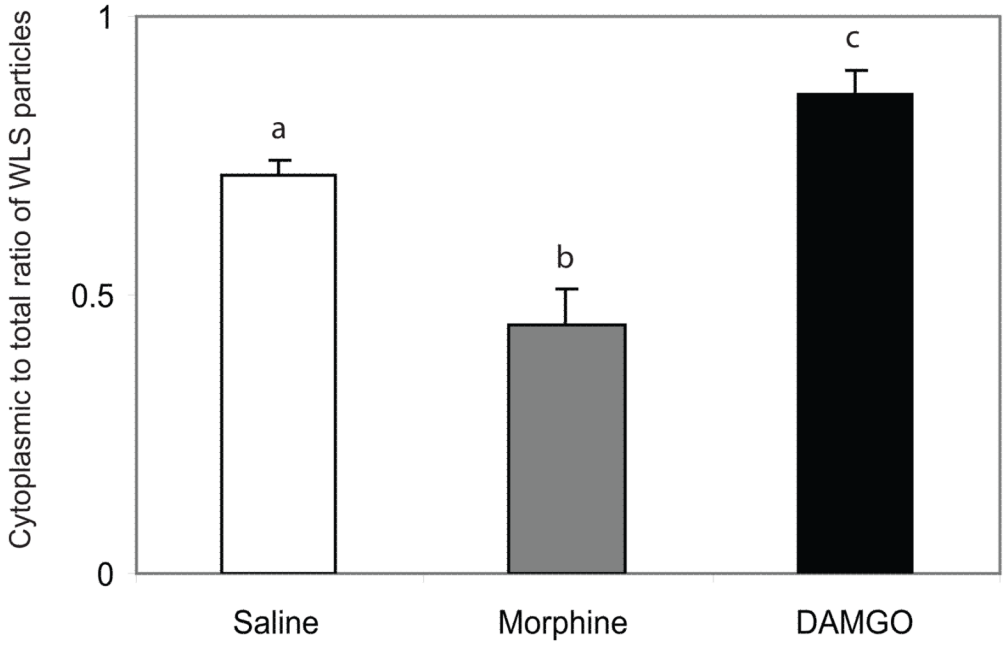

Figure 3.

Ratio of cytoplasmic to total WLS immunogold-silver particles following opioid agonist treatment. Morphine treatment caused a significant ($P<0.0001$) shift in WLS distribution from the cytoplasmic compartment to the plasma membrane. DAMGO treatment significantly increased ($P<0.0001$) the ratio of cytoplasmic to total immunogold-silver particles compared to saline- (control) and morphine-treated rats. Values are means ± SEM of three rats per group. Values with different letters are significantly different from each other. Tukey's multiple comparison test after ANOVA.

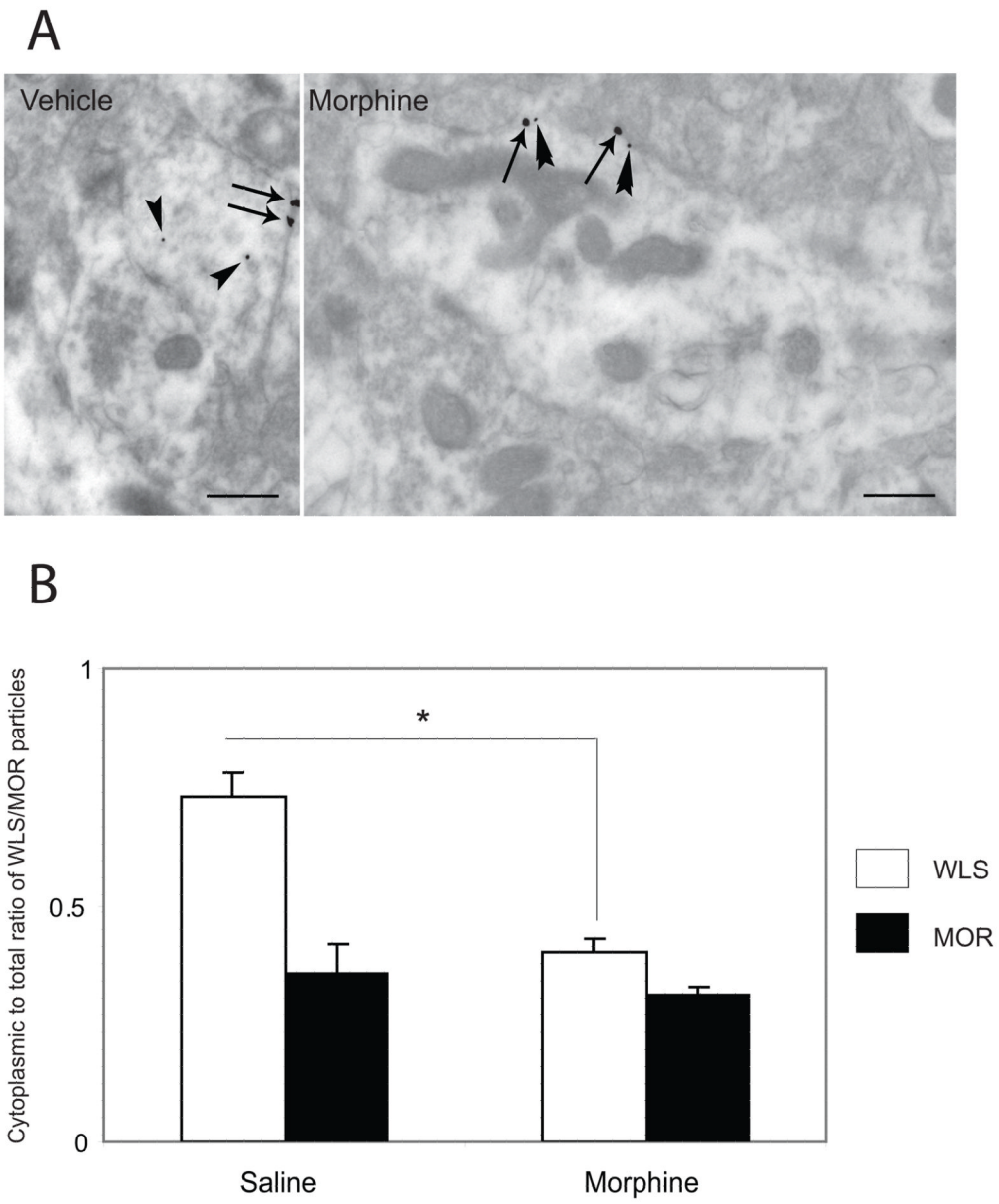

Figure 4.

A. Electron microscopic evidence for agonist-induced trafficking of WLS in rat striatum. Section from control (vehicle-treated) shows small gold-silver grains for WLS (arrowheads) and large gold-silver grains for MOR (arrows) in a common striatal dendrite. WLS immunolabeling is localized within the cytoplasm while MOR immunolabeling is localized along the plasma membrane of the striatal dendrite. Following morphine treatment, MOR immunolabeling is consistently localized along the plasma membrane (arrows) while WLS immunolabeling shows a shift in distribution from the cytoplasm to the plasma membrane (double arrowheads). **B.** Ratio of cytoplasmic to total WLS and MOR immunogold-silver particles following morphine treatment. Morphine treatment caused a significant ($P<0.05$) shift in WLS distribution from the cytoplasmic compartment to the plasma membrane compared to saline- (control) rats. * $P<0.05$ saline-(control) rats following Student's *t*-test.

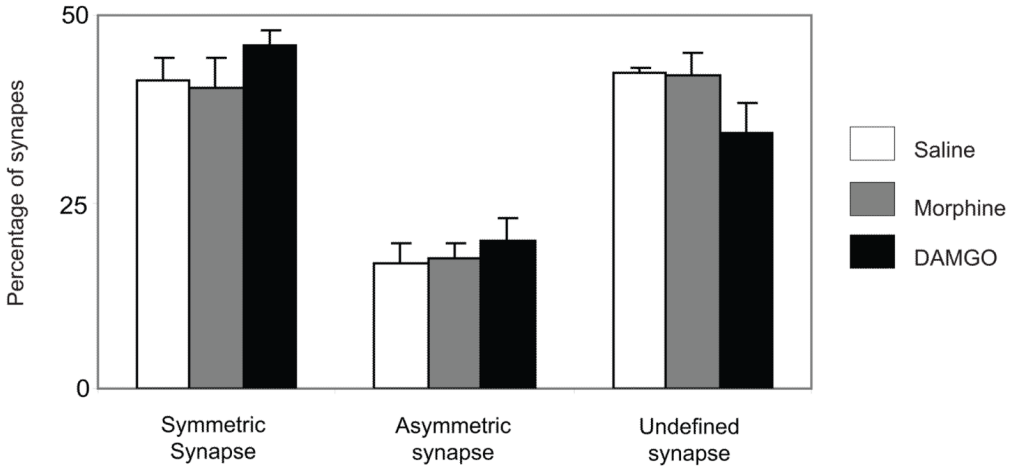

Figure 5.

Percentage of type of synaptic specialization received by WLS-containing dendrites. There was no significant difference in the type of synapses formed between the three groups analyzed. Values are means ± SEM of five rats per group. (ANOVA).

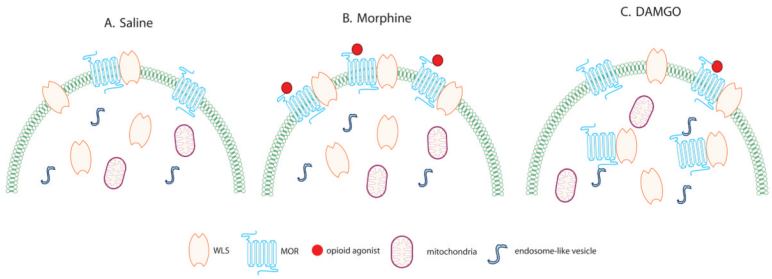

Figure 6.

Schematics depicting the potential cellular interaction and trafficking of WLS and MOR in rat striatal processes following opiate agonist treatment. **A.** Following saline treatment, WLS and MOR are associated with the plasma membrane while most WLS are localized within the cytoplasm. **B.** Following morphine treatment, the binding of morphine to MOR causes more WLS and MOR to translocate to the plasma membrane. **C.** Following DAMGO treatment, WLS and MOR remain within the cytoplasm where they are often associated with endosome-like vesicles.

Table 1

Total number of WLS-immunogold silver particles in striatal dendrites

	Dendrites
Vehicle	319.20 ± 9.65
Morphine	346.40 ± 62.63
DAMGO	390.00 ± 58.54

Values are means ± SEM.

Number of WLS-immunogold silver particles in intracellular compartment of dendrites in the striatum

Table 2

	Dendrites
Vehicle	226.40 ± 7.40[a]
Morphine	157.20 ± 19.20[b]
DAMGO	334.60 ± 48.15[c]

Values are means ± SEM of five rats per group. Values with different letters are significantly different from each other (* $P < 0.0001$). Tukey-Kramer multiple comparisons test after ANOVA.